Title
The Epitaxial Growth of Zirconium Oxide Thin Films on Pt(111) Single Crystal Surfaces

Authors
Maurice, V.
Salmeron, E.M.
Somorjai, Gabor A.

Publication Date
1990-08-01

LBL-28699
Preprint

Center for Advanced Materials

CAM

Submitted to Surface Science

The Epitaxial Growth of Zirconium Oxide Thin Films on Pt(111) Single Crystal Surfaces

V. Maurice, M. Salmeron, and G.A. Somorjai

August 1990

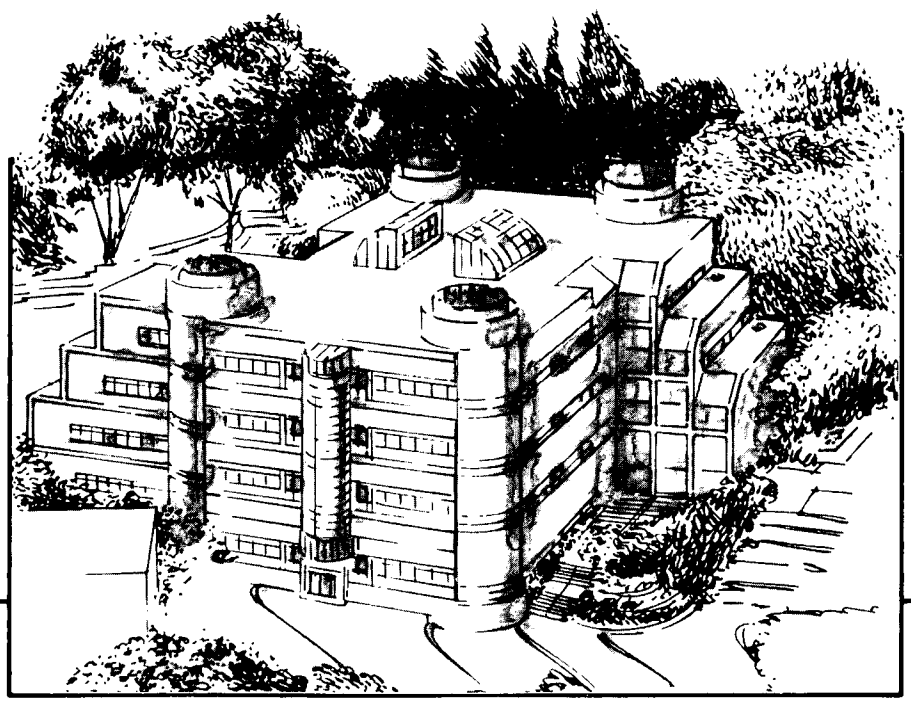

Materials and Chemical Sciences Division

Lawrence Berkeley Laboratory • University of California

ONE CYCLOTRON ROAD, BERKELEY, CA 94720 • (415) 486-4755

Prepared for the U.S. Department of Energy under Contract DE-AC03-76SF00098

DISCLAIMER

LBL-28699

The epitaxial growth of zirconium oxide thin films on Pt(111) single crystal surfaces

V. Maurice*, M. Salmeron and G.A. Somorjai

Department of Chemistry
University of California
and
Center for Advanced Materials
Materials and Chemical Sciences Division
Lawrence Berkeley Laboratory
1 Cyclotron Road
Berkeley, CA 94720

* Permanent address:
Laboratoire de Physico-Chimie des Surfaces
UA 425 - Universite Paris VI
Ecole Nationale Superieure de Chimie de Paris
11 rue Pierre et Marie Curie
75231 Paris Cedex 05, France

Acknowledgement

This work was supported by the Director, Office of Energy Research, Office of Basic Research, Materials Science Division of the U.S. Department of Energy under Contract No. DE-AC03-76F00098.

Abstract

Zirconium oxide films were deposited onto a Pt(111) surface by resistively heating a Zr wire under oxidative conditions. The composition and structure of the surface was determined by AES, ISS, XPS and LEED. Below 700K, the growth of the oxide films is 2D up to the completion of a monolayer. Zr is in the 3+ oxidation state. Upon brief annealing above 900K in oxidative conditions, ordered ZrO_2 films are formed with the fcc structure of bulk ZrO_2. The (111) planes of the ZrO_2 films grow parallel to the (111) subtrate plane. Multilayer ordered films can be grown with a thickness of at least 7 monolayers, although with a substantial amount of defects. Upon extensive annealing above 1100K in oxidative conditions, a different ordered structure is produced which is the result of the reduction and dissolution of the oxide films into the Pt subtsrate. It is related to the structure of the interface between the zirconium oxide films and the Pt substrate.

1. Introduction

Oxide surfaces have tremendous chemical and mechanical importance in determining the chemical as well as the tribological properties of many systems. Zirconium oxide is of great interest as a hard protective coating for thin film data storage media. When covered with perfluorinated polyethers, the system offers remarkable properties for the protection and lubrication of magnetic media. In order to study the chemisorption properties of oxide surfaces, oxide thin films may be grown on ordered metallic substrates. It is expected that the properties of epitaxially grown films can be controlled by changing the nature and/or the structure of the metallic substrate. Besides, thin film studies allow to overcome the difficulties of preparing and cleaning single crystal of oxides and eventually, the difficulties of charging which may be encountered due to insulating properties. This paper reports the growth of zirconium oxide thin films on a platinum (111) substrate.

Many approaches could be used in order to grow thin films of metal oxides on a metal substrate. One of them is to grow the metal oxide films on a similar metal substrate. Because of its importance in nuclear technology, the surface properties of metallic zirconium have been extensively

studied. In particular, much effort has been made to study the initial stages of its oxidation [1-10]. It appears from these studies that oxide films can be grown at room temperature under oxygen exposure. In such conditions, the limiting thickness of the films has been estimated to be of 1.5-2 nm [1,3,6,10]. However, two major problems have been encountered in these studies. One is the difficulty to produce clean Zr surfaces as sulfur and chlorine have been found to be the two major surface contaminants of bulk zirconium [4,9]. The other is associated with the production of suboxides during the initial stages of the oxidation [2,5,7,10] which may cause significant deviations of stoichiometry with the increasing thickness of the oxide film.

In this study, a different approach has been selected which is to grow the metal oxide film on a dissimilar metal substrate. This approach has already been successfull in a few cases [11-16]. Bardi, Ross and Somorjai have reported a study of the deposition of Zr on a Pt(100) substrate and its reaction with oxygen and carbon monoxide [11,12]. Several metastable ordered structures are observed when oxidized overlayers are annealed, and protracted annealing above 900K results in the reduction and dissolution of the oxidized zirconium with complete disappearance of Zr from the surface. However, oxygen dosing of these annealed surfaces causes the segregation of Zr to the surface. A similar behaviour as a function of temperature has been reported for TiO_2 supported on polycrystalline Pt [17-19]. Studies of Zr and O co-adsorption on W(100) have also been reported [20,21]. In this case, it was found that deposition of Zr onto W(100) followed by heating in an oxygen partial pressure causes the diffusion of Zr-O complex into the bulk and the formation of a tungsten oxide layer. Heating in vacuum causes desorption of the tungsten oxide and segregation of the Zr-O complex to the surface. In view of the highly exothermic heat of formation of zirconium intermetallic compounds, it is not surprising that Zr bulk diffusion has been found to take place in these studies. This is the major difficulty to overcome when growing zirconium oxide films on dissimilar metal substrates. In both these studies, conditions are reported for which zirconium oxide is found to segregate to the metal surface. It can be expected then that in such conditions, thin films of zirconium oxide can be grown on the substrate and be thick enough so that eventual Zr bulk diffusion would affect only the zirconium oxide interface with the metal substrate and not the external

zirconium oxide surface.

A Pt(111) substrate has been selected in order to attempt to grow epitaxial thin films of zirconium oxide. The surface sensitive techniques used were Auger Electron Spectroscopy (AES), Low Energy Electron Diffraction (LEED), Ion Scattering Spectroscopy (ISS), X-ray Photoelectron Spectroscopy (XPS) and Thermal Desorption Spectroscopy (TDS). Epitaxial thin films of ZrO_2 have been grown with a thickness estimated to be about 10 monolayers. A substantial amount of defects is present in these thick films.

2. Experimental

This ultra high vacuum (UHV) study was performed in a standard system with a base pressure of $2x10^{-10}$ Torr. The system has been described in detail previously [14,16]. In the AES experiments the modulation voltage was 3 V peak to peak. A primary beam with an energy of 1.5 keV was used. Typical crystal currents of 6 μa were used. The XPS spectra were obtained using a Mg Kα x-ray source. Peak positions were assigned by setting the Pt $4f_{5/2}$ and Pt $4f_{7/2}$ peaks at 74.25 eV and 70.9 eV binding energy respectively. ISS experiments could be performed by a simple modification of the double pass cylindrical mirror analyser [16,22]. The primary ion beam consisted of 500 eV He^+ ions. The approximate scattering angle was 148°. Under these conditions ISS is only sensitive to the outermost atomic layer. A UTI mass spectrometer was used for the TDS experiments. The mass spectrometer was encapsulated except for a protruding 2 mm diameter aperture. Exposures were measured in Langmuirs ($1L=10^{-6}$ Torr. s) without corrections for the ion gauge sensitivity. Temperatures were measured using a chromel alumel thermocouple directly spotwelded to the platinum single crystal.

The zirconium evaporation source used in this study consisted of a high purity (99.99%) 25 mil diameter zirconium wire that was resistively heated. The platinum crystal was at a distance of about 25 mm during evaporation. Sulfur and chlorine were found to be major contaminants in a new source. However, outgassing of the source for about 15 hours at currents slightly below the

evaporation current was effective in eliminating these contaminants. The zirconium oxide films were deposited on the Pt(111) substrate by evaporating zirconium in a $5x10^{-7}$ Torr oxygen partial pressure. This method was found to be much more effective in producing carbon free oxide films than zirconium deposition in UHV conditions with subsequent oxygen dosing. After each deposition, the surface was annealed below 700K for a few seconds. In order to produce long range structural order of the deposited films, annealing treatments above 900K were necessary. However, extensive annealings resulted in the reduction and the dissolution of the oxide films into the substrate even when oxidative conditions were maintained in the chamber.

3. Results and Discussion

3.1. Coverage determination of zirconium oxide films on Pt(111)

The coverage of the zirconium oxide films deposited on Pt(111) has been monitored by AES, ISS and carbon monoxide titration with TDS. The monolayer completion has been calibrated with ISS and TDS in conditions where no dissolution of the oxide films into the metal substrate takes place.

ISS probes only the outermost layer of the surface. Consequently, the ISS Pt signal is proportional to $1-\theta$, θ being the fractional coverage of the zirconium oxide film. Figure 1 shows a plot of the ISS Pt signal vs. the AES Zr 113 eV to Pt 237 eV peak to peak height ratio. A steep decrease of the ISS Pt signal is measured up to an AES ratio of 1.8. The Pt signal is then 7% of that of the clean surface. Beyond this AES ratio, a slowly decreasing ISS Pt signal is measured. This residual signal is probably due to substrate spots which are not completely covered by the 2D oxide overlayer as the second oxide layer starts growing before the completion of the first one. The AES ratio of 1.9 ± 0.1 is assigned to correspond to one momolayer of zirconium oxide.

It is known from previous UHV experiments that carbon monoxide does not adsorb on

zirconium oxide [12] whereas it does on platinum. Consequently, the CO intensity signal recorded in a TDS experiment after dosing with CO a partially covered Pt substrate is proportional to the area uncovered by the oxide film. CO TDS spectra have been recorded after dosing surfaces of different oxide coverages with 30L of CO at 300K. Figure 2 shows a plot of the TDS CO signal intensity vs. the AES Zr 113 eV to Pt 237 eV peak to peak height ratio. The onset of the CO signal corresponds to an AES ratio of 2.0±0.1. This value is again associated with the completion of 1 monolayer of zirconium oxide and agrees with the value deduced from the ISS measurements.

AES uptake curves have been obtained by measuring the Auger peak to peak heights of the Zr 113 eV and Pt 237 eV signals as a function of the deposition time. They are shown in fig. 3. ISS and TDS measurements are used to assign a first break at 18 minutes deposition time for which the AES Zr 113 eV to Pt 237 eV peak to peak height ratio is 1.9. At the monolayer completion, the attenuation of the Pt 237 eV signal is 48% in agreement with the value reported on Pt(100) (47%) [12] and with typical attenuation values [14,23]. Using the classic attenuation expression [23]:

$$I_S/I^0_S = \exp (- d / 0.75 \times \lambda) \qquad (1)$$

one obtains a value of 2 monolayers for λ, the inelastic mean free path of 237 eV electrons. Although the curves show some scatter, we assign a second break to a 36 minutes deposition time. The Pt 237 eV signal is then attenuated another 61%. Although this seems to support this second assignment, the scattering of the data points in the Auger uptake curve is large.

On the basis of AES uptake curves, Bardi and Ross have concluded a layer-by-layer (Frank van der Merwe type) growth mode for zirconium oxide films on Pt(100) [12]. They report a first break for an AES Zr 113 eV to Pt 237 eV peak to peak height ratio of 1.8 and a Pt 237 eV signal attenuation of 47%, in agreement with our results. These authors have been able to assign a second break with another 47% Pt 237 eV signal attenuation. The excellent agreement between both studies up to the completion of the first monolayer may indicate that the growth mechanism is also of Frank van der Merwe type in our case.

3.2. Structure of zirconium oxide films on Pt(111).

Clean Pt(111) gives a p(1x1) LEED pattern characteristic of the bulk platinum periodicity. It is shown on fig. 4a. The reciprocal unit vectors (i.e. the shortest distance between two substrate spots) correspond to a 2.77Å distance between Pt atoms in real space. Deposition of zirconium oxide ranging from submonolayer to multilayer coverages followed by annealing below 700K produces an increase of the background intensity and a decrease of the intensity of the substrate spots as the coverage is increased. This is characteristic of the absence of long range structural order. Annealing at temperatures above 900K causes the appearance of new LEED patterns shown in fig. 4b, c and d. Two basic structures are observed that are denoted I (fig.4b) and II (fig.4c and d). Their appearance depends on the annealing conditions which cause eventually the reduction and the dissolution of the oxide films into the Pt substrate. These structures will be separately discussed in the next subsections.

3.2.1. The $(^{8/3}{}_{0}{}^{0}{}_{8/3})$ superstructure.

Annealing of freshly deposited films ranging from submonolayer to multilayer coverages for a few seconds between 900 and 1100K in oxidizing conditions ($5x10^{-7}$ Torr of O_2) causes the appearance of structure II. The LEED pattern for multilayer coverage is shown in fig. 4d and a schematic representation with substrate spots is given in fig. 5a. The superstructure unit cell is denoted p(8/3x8/3) in Wood's notation or $(^{8/3}{}_{0}{}^{0}{}_{8/3})$ in matrix notation. The real space unit vectors are 7.4Å long and separated by 120°. At low coverages, the spots of structure II coexist with Pt substrate spots. As the coverage is increased, the intensity of the substrate spots decreases and that of the superstructure spots increases. Eventually, the substrate spots become undetectable for multilayer coverage as shown in fig. 4d. In this case, a complete attenuation of the low energy Auger Pt peaks is also measured. For all coverages, the superstructure spots are broad and the background intensities are high which indicates a substantial amount of disorder. It is interesting to notice that the

hatched spots shown in fig.5a, corresponding to a p(4/3x4/3) superstructure are always more intense than the spots corresponding to the p(8/3x8/3) superstructure. The measurements associated with structure II are summarized in table 1.

No significant variations of the AES Zr 113 eV to Pt 237 eV ratio are measured after the annealing treatment. Also, the ISS spectrum is unchanged as shown in fig. 6. This indicates that no measurable reduction and dissolution of the zirconium oxide films has occured. The XPS measurement of the binding energy of the Zr $3d_{5/2}$ core level is characteristic of a Zr^{4+} oxidation state (see section 3.3). Consequently, this structure corresponds to clean and ordered ZrO_2 thin films although with a significant amount of defects.

Four different structures have been reported for bulk ZrO_2 with orthogonal, face centered cubic, monoclinic and tetragonal lattices [25]. The variation of the lattice parameters between these different structures is at most 6%. The fcc crystalline form has the calcium fluoride structure. The unit vector in the (111) planes of hexagonal symmetry is 3.6Å. Half the unit vector of superstructure II (3.7Å) represents an extension of 3% with respect to the 3.6Å value. Taking into account this relationship, the (111) planes of the fcc structure of ZrO_2 form a p(4/3x4/3) superstructure with respect to the Pt (111) planes. One can consider the p(8/3x8/3) superstructure as corresponding to a p(2x2) superstructure with respect to (111) planes of the calcium fluoride structure of ZrO_2. This is supported by the significant difference between the intensities and shapes of the p(4/3x4/3) spots and those of the p(8/3x8/3) spots of the LEED pattern shown in fig. 4d.

In the fcc structure of ZrO_2, the (111) planes contain either O atoms only or Zr atoms only and have equal density. The stacking sequence alternates two O planes for one Zr plane. The O atoms sit in threefold hollow positions with respect to the Zr(111) planes. A p(2x2) superstructure with respect to these (111) planes could result from the distribution of 25% of O vacancies in a surface O(111) plane. Electron beam induced changes of insulator surfaces are known to be significant [26-30] and it is possible that electron stimulated oxygen desorption occured during electron spectroscopy experiments (LEED and AES). According to this model, the measurement of both Zr and O signal in the ISS spectra corresponding to structure II can be explained if one

considers the low packing density of the (111) planes of the fcc structure of ZrO_2. The distance between two nearest neighbor atoms is 3.6Å; the Zr^{4+} and O^{2-} diameters are 1.6Å and 2.54Å respectively. The low packing density can thus make the two topmost surface layers accessible to the He^+ ions.

The broad superstructure spots of the LEED pattern indicate that the films are probably made of patches of epitaxially grown oxide films whose average width is smaller than the coherence width of the LEED diffractometer. It is likely that these patches are packed so that the entire substrate surface is covered. Taking into account the complete attenuation of the AES Pt 237 eV signal intensity by the oxide multilayers, the thickness of the films can be estimated from eq. (1). A 99% attenuation gives a thickness of 7 monolayers. For 99.9%, the value becomes 10 monolayers.

Annealing of structure II for several minutes above 1100K in the same oxidizing conditions results in the appearance of a LEED pattern corresponding to the superposition of the patterns associated with stuctures I and II. Protracted annealing results in the increase of the intensity of the spots associated with structure I and the decrease of the intensity of the spots associated with structure II. When this structure is produced starting from a monolayer coverage, annealing above 1100K for several minutes in more severe oxidizing conditions ($2x10^{-5}$ Torr of O_2) results in the observation of the LEED pattern shown on fig. 4c. The superstructure is the same as in fig. 4d. However, the superstructure spots are much sharper and the background intensity is lower which indicates a more ordered structure. A decrease of the AES Zr 113 eV to Pt 237 eV peak to peak height ratio (from 2 to 0.6) and an increase of the AES O 508 eV to Zr 113 eV peak to peak height ratio (from 3 to 4.1) are measured. The ISS Pt signal becomes detectable. However, the ISS O to Zr ratio is unchanged. These measurements may indicate a 3D restructuring of the oxide patches (possibly a sintering like effect).

3.2.2. The $(^{1.16}_{\overline{0.26}}{}^{0.81}_{1.37})$ superstructure.

Annealing of a freshly deposited monolayer of zirconium oxide for several minutes above

1100K in an oxygen partial pressure of $5x10^{-7}$ Torr causes the appearance of structure I. The LEED pattern is shown in fig. 4b and a schematic representation is shown in fig. 5b. In order to elucidate the superstructure responsible for the many spots observed, some of them have been assigned to double diffraction from first order substrate spots. This is supported by calculations which reveal that the energy associated with a parallel momentum equal to the (1,1) vector is 48 eV, which is less than the primary energy used of 57 eV. The pattern is interpreted as resulting from the superposition of six different sets of spots. Each set corresponds to a low symmetry superstructure denoted $(^{1.16}_{\overline{0.26}}\ ^{0.81}_{1.37})$ in matrix notation. The real space unit cell vectors are 3.4Å long and are separated by 96.2±0.5°. Clearly, this indicates an incommensurate registry with the substrate.

The measurements associated with this structure are summarized in table 1. After annealing, a decrease of the AES Zr 113 eV to Pt 237 eV peak to peak height ratio and an increase of the AES O 508 eV to Zr 113 eV peak to peak height ratio are measured. Also, ISS measurements show the appearance of the Pt signal which was not detectable after deposition (see fig. 6). These results are obtained whatever the oxygen partial pressure in the chamber up to $5x10^{-5}$ Torr. This is the evidence of the reduction and of the dissolution of the oxide film into platinum. The oxidation state of the diffusing Zr has not been resolved with our XPS spectrometer.

We believe that this ordered structure is related to the interface between the oxide film and the Pt substrate. Bardi, Ross & Somorjai have reported a low symmetry superstructure denoted $(^{0.77}_{\overline{0.57}}\ ^{0.77}_{0.92})$ with respect to the Pt(100) unit vectors [11]. The superstructure unit vectors are in this case 3.00Å long and separated by 76.8°. The corresponding AES Zr 113 eV to Pt 237 eV peak to peak height ratio ranges from 1.4 to 2.6 and the AES O 508 eV to Zr 113 eV peak to peak height ratio is about 2. The fact that both superstructures are associated with similar AES Zr to Pt ratios may suggest that similar phases have been formed on both substrates. The differences in the structural parameters would indicate then the influence of the substrate structure due to epitaxial effects. The differences in the AES O to Zr ratios would suggest different stoichiometries. Stucture I could result either from the dissolution of metallic zirconium or reduced zirconia in the near surface Pt layers or from the mixing of platinum with the surface zirconium oxide as indicated by the Pt signal in the ISS

spectra. It may also correspond to the initial stages of growth of a mixed oxide ternary phase. A ternary phase between Pt and group IIIb metal oxides, $PtYO_{3.5}$, has been reported [24]. Although, we have not been able to find any ternary phase with group IVb metal oxides, one might expect surface Pt Zr_xO_y phases to form.

When structures I and II are produced simultaneously by extensive annealing of multilayer films having the structure II, a decrease of the AES Zr 113 eV to Pt 237 eV peak to peak height ratio and an increase of the AES O 508 eV to Zr 113 eV peak to peak height ratio are recorded. However, no Pt ISS signal is detectable afterwards nor changes of the O to Zr ISS ratio. This indicates that the topmost layer of the film is unchanged and that the interface between the oxide film and the substrate is mainly affected.

Finally, whenever dissolution of an oxide film into bulk platinum is produced, leaving the sample for a few hours in UHV or dosing with oxygen at room temperature causes the increase of the AES Zr 113 eV to Pt 237 eV peak to peak height ratio and the decrease of the the AES O 508 eV to Zr 113 eV peak to peak height ratio. Under these conditions Zr is driven back to the surface as a result of its strong affinity for oxygen.

Bardi, Ross & Somorjai have reported the dissolution into Pt(100) starting from 700 K for deposited metallic Zr and from 900K for deposited zirconium oxide [11]. A similar behaviour has been reported for the Zr/W(100) system [21]. Taking into account the highly negative free energy of solution for Zr into Pt, these observations are not surprising. The higher temperature necessary to dissolve zirconium oxide films probably result from the highly activated process of breaking very stable Zr-O bonds. These authors have also reported that dissolved Zr could be segregated to the topmost surface layers by annealing at high temperatures (above 900K) in oxidative conditions. This is in disagreement with our results as we found that annealing zirconium oxide films in these conditions causes the dissolution of the oxide films into the substrate instead of preventing it. We have observed surface segregation of dissolved zirconium when the crystal was left for a few hours under UHV conditions at room temperature (although with residual zirconium oxide on the surface) or, when the crystal was dosed extensively with oxygen still at room temperature.

The reduction and the dissolution of the oxide film into the Pt substrate and its segregation back to the surface may depend not only on the reducing or oxidizing conditions maintained in the chamber, but also on other parameters such as the amount of Zr previously dissolved, the solubility limit of Zr in the near surface region of the substrate, the diffusion rate of Zr, the structure, composition and thickness of the zirconium oxide platinum interface and of the oxide films. Most of these parameters are hardly contollable so that the extent of Zr dissolution upon annealing treatments depends on the history of the sample. As we were mainly interested in characterizing the structure and composition of thick oxide films, we have not concentrated our effort in a careful and detailed analysis of the interface of the oxide films with the Pt substrate. Such a study would probably explain the discrepancies about the Zr dissolution and segregation between our results and the ones reported by Bardi, Ross and Somorjai.

3.3 Stoichiometry of zirconium oxide films on Pt(111)

The stoichiometry of the zirconium oxide films has been studied with AES, ISS and XPS measurements which are summarized in table 1. No significant variations of the AES Zr 113 eV peak shape has been recorded in the range of stoichiometries studied. This is expected for this MNN Auger transition which does not involve valence electrons. For freshly deposited zirconium oxide films, the AES O 508 eV to Zr 113 eV peak to peak height ratio ranges from 2 at monolayer coverage to about 3 at multilayer coverage. The ISS oxygen to zirconium ratios are 0.5 and 0.7 at monolayer and multilayer coverage respectively. The Zr $3d_{5/2}$ core level binding energy measured by XPS is 181.9 eV at multilayer coverage. For structure I produced by annealing films of about 1 monolayer coverage in oxidizing conditions, the AES O 508 eV to Zr 113 eV peak to peak height ratio increases to values of about 3 typically. The ISS ratio is also found to increase to values of about 0.6. The Zr $3d_{5/2}$ core level binding energy is 182.3 eV. For structure II, the AES O 508 eV to Zr 113 eV peak to peak height ratio ranges from 2.8 to 3.7. The corresponding ISS ratio is about 0.7. The Zr $3d_{5/2}$ core level binding energy is 182.8 eV.

The binding energy of the Zr $3d_{5/2}$ core level for the multilayer films associated with structure II (182.8 eV) agrees remarkably with that of the Zr^{4+} oxidation state reported in the literature: 182.75 ev [10], 182.9 eV [7]. The AES O 508 eV to Zr 113 eV peak to peak height ratio associated with these multilayer ordered films is ranging from 3.4 to 3.7. We propose that this range corresponds to the ZrO_2 stoichiometry under our measurement conditions.

When structure I was produced, the binding energy of the Zr $3d_{5/2}$ core level was 182.3 eV. Accordingly, we measured a lower AES O 508 eV to Zr 113 eV peak to peak height ratio value of about 3 and a lower ISS oxygen to zirconium ratio also. The shift of 0.5 eV of the binding energy of the Zr $3d_{5/2}$ core level indicates a lower oxidation state of zirconium. Suboxide structures have been reported by different authors which shift from the Zr^0 oxidation state (178.7 eV) by 1 and 2 eV [7], 1.2 and 3.3 eV [8], and 2 eV [2]. An energy shift of about 1.1 eV per Zr-O bond has been proposed to explain the suboxide structures [10]. The shift value of 0.5 eV recorded for structure I (with respect to ZrO_2) still differs significantly from the value of 1.1 eV to suggest a Zr^{3+} oxidation state.

For freshly deposited multilayers of zirconium oxide, the Zr $3d_{5/2}$ core level binding energy is 181.9 eV. A shift of 0.9 eV results when such layers are annealed to produce structure II associated with the ZrO_2 stoichiometry. Clearly, this indicates that the ZrO_2 stoichiometry is not reached after deposition of the films, and that annealing is necessary in order to maximize the coordination of zirconium with O atoms. The 181.9 eV value of the Zr $3d_{5/2}$ core level binding energy suggests a Zr^{3+} oxidation state. This is in agreement with some suboxides structures reported from the oxidation of bulk zirconium and fit reasonably the 1.1 eV shift estimated per Zr-O bond [10]. The variation of the AES O 508 eV to Zr 113 eV peak to peak height ratio associated with the annealing treatments reflects the stoichiometry variation. However, the ISS O to Zr signal ratio does not vary significantly (about 0.7) indicating that the stoichiometry variations affect mostly the near surface layers but not the outermost layer.

5. Summary

Epitaxial thin films of zirconium oxide have been grown onto a Pt(111) metal substrate. The films are stable under UHV conditions. Thicknesses of at least 7 monolayers have been reached without any difficulty. The main findings from this work are:

1/ Below 700K, zirconium oxide grows essentially 2D up to the near completion of one monolayer. The AES Zr 113 eV to Pt 237 eV peak to peak height ratio is then 1.9±0.1. O and Zr atoms are present in the topmost layer. XPS measurements indicate a Zr^{3+} oxidation state.

2/ Annealing above 900K is necessary in order to produce long range structural order of the zirconium oxide films. Extensive annealing however causes the reduction and the dissolution of the oxide films into the Pt substrate despite the oxidative conditions maintained in the chamber. The oxidation state of the diffusing Zr has not been resolved. Zr diffuses back from the subtrate bulk to surface in oxidative conditions below 700K.

3/ Ordered thin films with ZrO_2 stoichiometry are produced by short time annealing above 900K. They have the fcc crystalline form of bulk ZrO_2 with the (111) crystallographic plane parallel to the substrate (111) plane and the crystallographic directions matching those of the substrate. The surface unit cell of the films is 2x2 times that of the bulk oxide The films can be grown from submonolayer to multilayer coverages up to thicknesses of at least 7 monolayers. A substantial amount of structural defects is observed at multilayer coverages. O and Zr are present in the outermost layers.

4/ Another ordered surface structure is produced by extensive annealing above 1100K of 1 monolayer of deposited oxide. It is associated with the structure of the interface between the oxide film and the Pt substrate. XPS measurements indicate a Zr oxidation state between 4+ and 3+. ISS measurements indicate that Pt, Zr and O atoms are present in the outermost layer.

Acknowledgements

This work was supported by the Director, Office of Energy Research, Office of Basic Research, Materials Science Division of the U.S. Department of Energy under Contract No. DE-AC03-76F00098. Additional support of the work was provided by a grant from IBM (Almaden Research Center). One of us (VM) would like to thank support from OTAN and NSF.

References

[1] R.L. Tapping, J. Nucl. Mater. 107(1982)151.

[2] P. Sen, D.D. Sarma, R.C. Budhani, K.L. Chopra and C.N.R. Rao, J. Phys. F 14(1984)565.

[3] J.M. Sanz, C. Palacio, Y. Casas and J.M. Martinez-Duart, Surface Interface Anal. 10(1987)177.

[4] G.B. Hoflund, G.R. Corallo, D.A. Asbury and R.E. Gilbert, J. Vacuum Sci. Technol. A 5(1987)1120.

[5] G.R. Corallo, D.A. Asbury, R.E. Gilbert and G.B. Hoflund, Phys. Rev. B 35(1987)9451.

[6] B. Jungblut, G. Sicking and T. Papachristos, Surface Interface Anal. 13(1988)135.

[7] C.O. de Gonzalez and E.A. Garcia, Surface Sci. 193(1988)305.

[8] L. Kumar, D.D. Sarma and S. Krummacher, Appl. Surface Sci. 32(1988)309.

[9] M. Tomita, T. Tanabe and S. Imoto, Surface Sci. 209(1989)173.

[10] C. Morant, J.M. Sanz, L. Galan, L. Soriano and F. Rueda, Surface Sci. 218(1989)331.

[11] U. Bardi, P.N. Ross and G.A. Somorjai, J. Vacuum Sci. Technol. A 2(1984)40.

[12] U. Bardi and P.N. Ross, Modification of the surface properties of metals by oxide overlayers: I. oxidized zirconium deposited on the Pt(100) single crystal surface. Technical Report, LBL-21772, 1986.

[13] W.T. Tysoe, F. Zaera and G.A. Somorjai, Surface Sci. 200(1988)1.

[14] G.H. Vurens, M. Salmeron and G.A. Somorjai, Surface Sci. 201(1988)129.

[15] K.J. Williams, M. Salmeron, A.T. Bell and G.A. Somorjai, Surface Sci. 204(1988)L745.

[16] G.H. Vurens, PhD Thesis, Rijksuniversiteit Leiden, 1989.

[17] C.S. Ko and R.J.Gorte, J. Catalysis 90(1984)59.

[18] C.S. Ko and R.J.Gorte, Surface Sci. 161(1985)597.

[19] R.J. Gorte, E.Altman, G.R.Corallo, M.R. Davidson, D.A. Ashbury and G.B. Hoflund, Surface Sci. 188(1987)327.

[20] L.R. Danielson and L.W. Swanson, Surface Sci. 88(1979)14.

[21] P.R. Davis, Surface Sci. 91(1980)91.

[22] G.B. Hoflund, D.A. Ashbury, P. Kirszensztejn and H.A. Laitinen, Surface Sci. 161(1985)L583.

[23] Practical Surface Analysis by Auger and X-ray Photoelectron Spectroscopy, Eds: D. Briggs and M.P. Seah, John Wiley & Sons, 1983.

[24] JCPDS Powder Diffraction File 21-1453.

[25] Pearson's Handbook of Crystallographic Data for Intermetallic Phases, Eds: P. Villars and L.D. Calvert, American Society for Metals,1986.

[26] J.S. Johannessen, Faraday Disc. Chem. Soc. 60(1975)313.

[27] M.L. Knotek, Surface Sci. 91(1980)L17.

[28] M.L.Knotek, Phys. Today 37(1984)24.

[29] K.O. Axelsson, K.E. Keck and B. Kasemo, Appl. Surface Sci. 25(1986)217.

[30] D.A. Ashbury, G.B. Hoflund, W.J. Peterson, R.E. Gilbert and R.A. Outlaw, Surface Sci. 185(1987)213.

Captions

Table 1: Summary of the AES, ISS, XPS and LEED measurements for the different zirconium oxide films deposited on Pt(111).

Figure 1: Variation of the ISS Pt signal intensity as a function of the AES Zr 113 eV to Pt 237 eV peak to peak height ratio. The ISS Pt intensity is normalized to the value recorded for the clean Pt(111) surface.

Figure 2: Variation of the CO TDS integrated signal intensity as a function of the AES Zr 113 eV to Pt 237 eV peak to peak height ratio.

Figure 3: Variation of the AES peak to peak height of the Zr 113 eV and Pt 237 eV signals as a function of the deposition time of the zirconium oxide. Breaks mark the deposition time for 1 and 2 monolayers according to the ISS and CO titration calibrations.

Figure 4: LEED patterns for: (a) clean Pt(111), 68 V; (b) structure I, 57 V; (c) stucture II, 65 V; (d) structure II, 65 V.

Figure 5: Schematic representation of the LEED pattern corresponding to structure II (a) and structure I (b). The superstruture unit cell is indicated. Black spots represent substrate spots. In (a), striped and white dots indicate the p(4/3x4/3) and p(8/3x8/3) spots respectively. In (b), striped and white dots indicate double diffraction spots and single diffraction spots respectively.

Figure 6: ISS spectra for: (a) clean Pt(111); (b) 1 monolayer of zirconium oxide after deposition; (c) 1 monolayer after annealing at 1150K for 5 minutes (structure I); (d) multilayers of zirconium oxide after deposition; (e) multilayers after annealing at 1050K for 30 sec. (structure II).

	Zr/Pt AES ratio	O/Zr AES ratio	O/Zr ISS ratio*	Zr $3d_{5/2}$(eV)	structure unit cell dim., Å angle of unit vectors
clean Pt(111)	0.0	------	------	------	p(1x1) 2.77 120.0°
1 monolayer after deposition	1.9	2.0-2.5	0.5	------	disordered
multilayers after deposition	>1.9	2.5-3.0	0.5-0.7	181.9	disordered
structure I	1.5-2.8	3.0	0.6	182.3	$(^{1.16}{}_{0.26}{}^{0.81}{}_{1.37})$ 3.4 96.2°
structure II.a	>1.1	2.8-3.7	0.7	182.8	p(4/3x4/3) + p(8/3x8/3) 3.7 ; 7.4 120.0°
structure II.b	0.6	4.1	0.7	------	p(8/3x8/3) 7.4 120.0°

* Ratios vary in a range around 10%

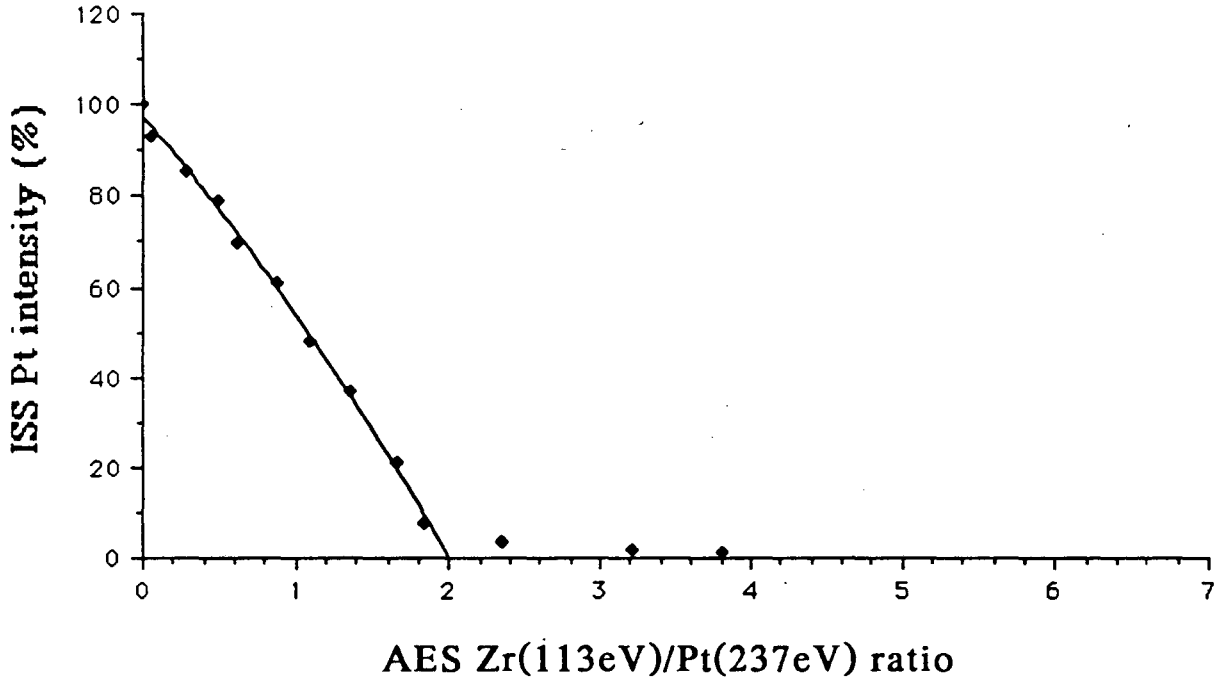
ISS Pt intensity (%)
120
100
80
60
40
20
0
0
1
2
3
4
5
6
7
AES Zr(113eV)/Pt(237eV) ratio

Fig. 1

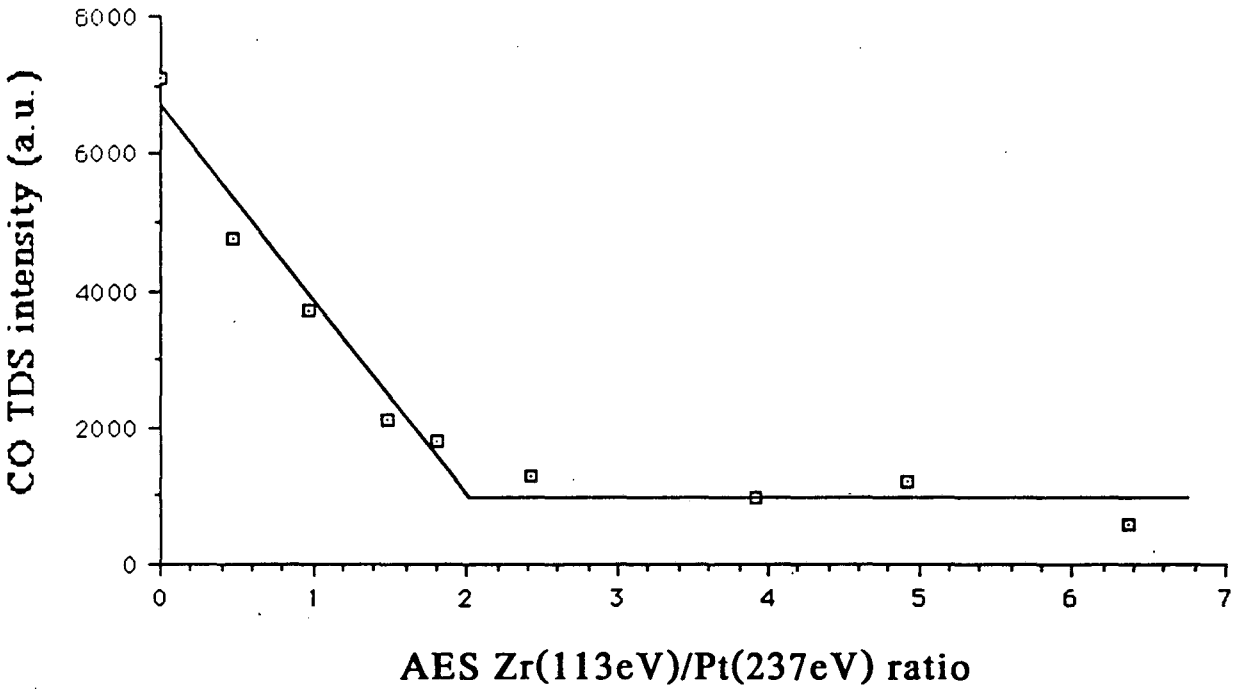
CO TDS intensity (a.u.)
8000
6000
4000
2000
0
0
1
2
3
4
5
6
7
AES Zr(113eV)/Pt(237eV) ratio

Fig. 2

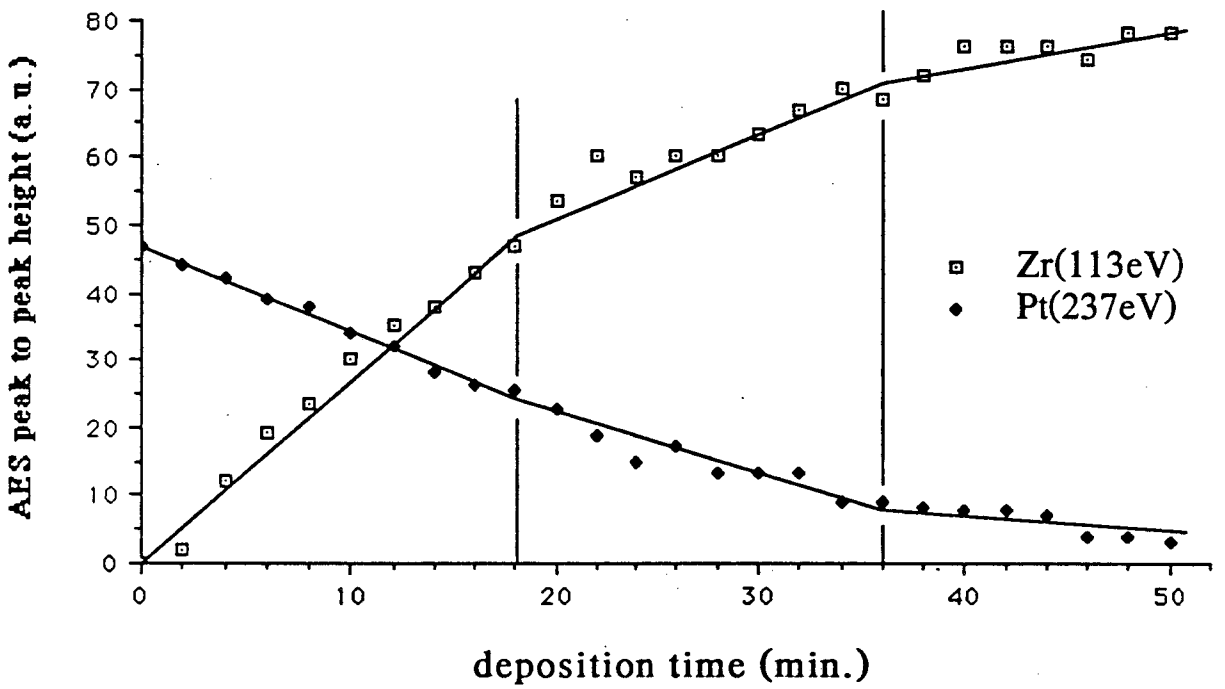
AES peak to peak height (a.u.)
80
70
60
50
40
30
20
10
0
0
10
20
30
40
50
deposition time (min.)
Zr(113eV)
Pt(237eV)

Fig. 3

a: Clean Pt(111) b: Structure I

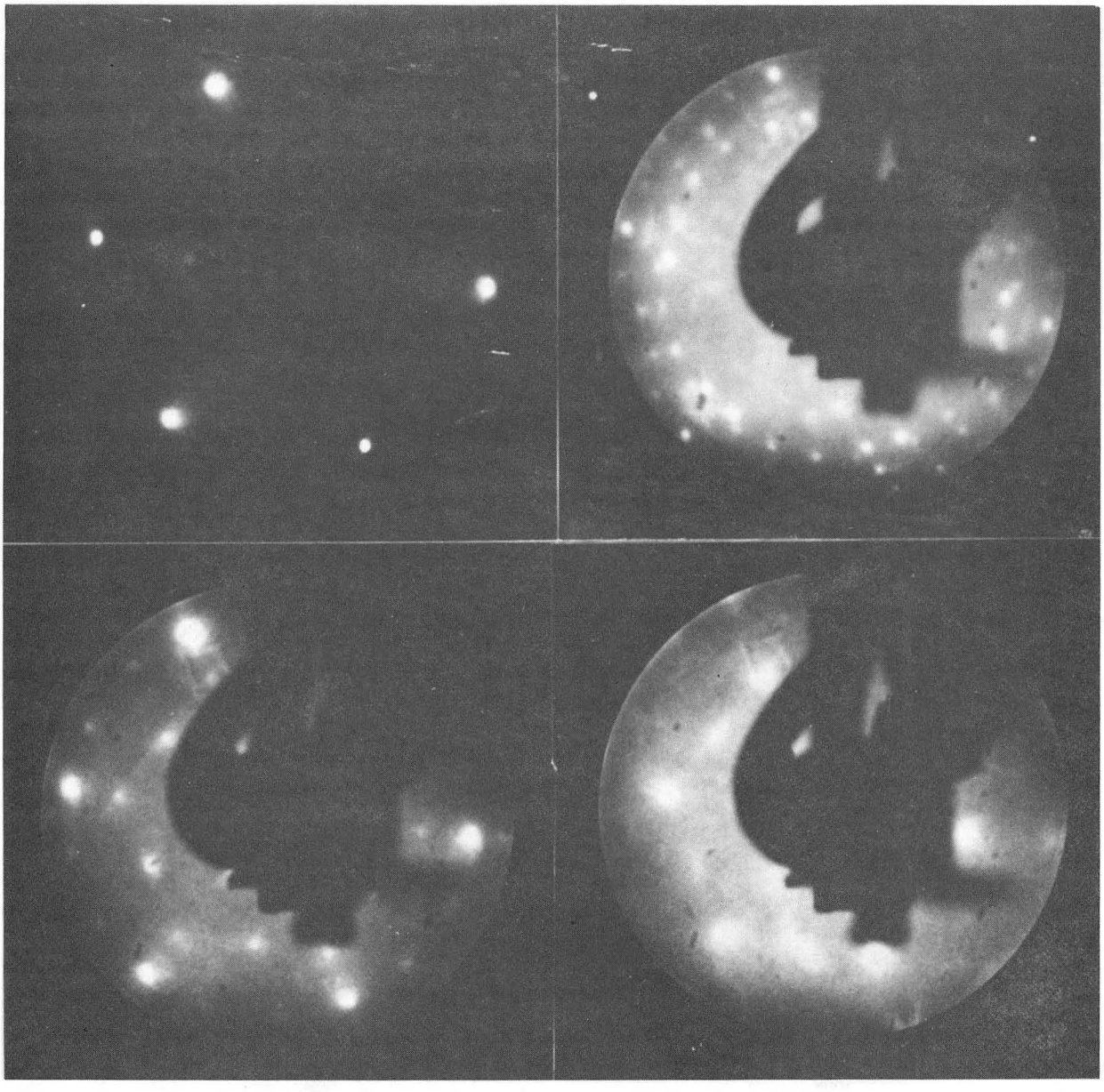

XBB902-1384

c: Structure II d: Structure II

Fig. 4

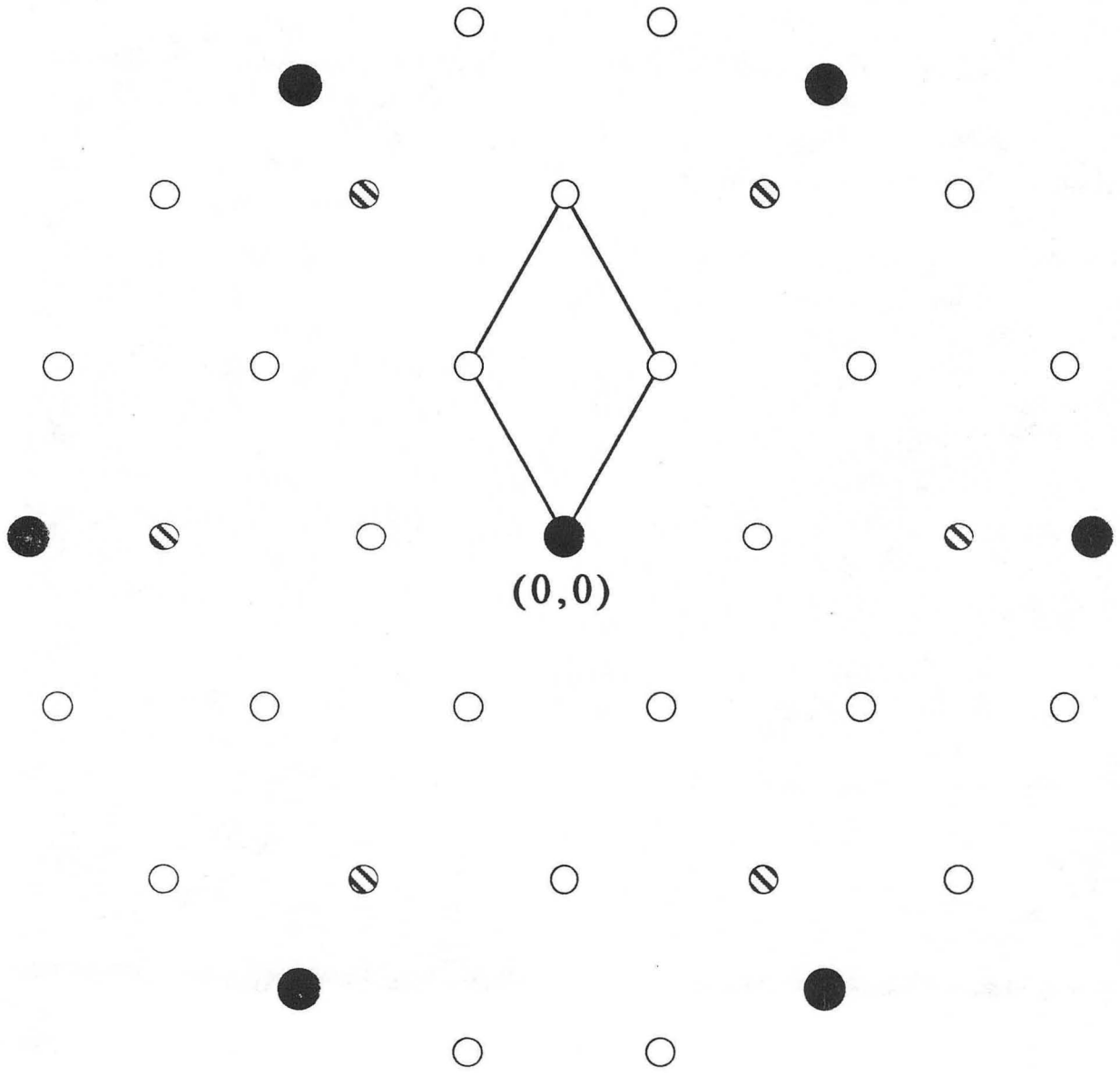

Fig. 5a

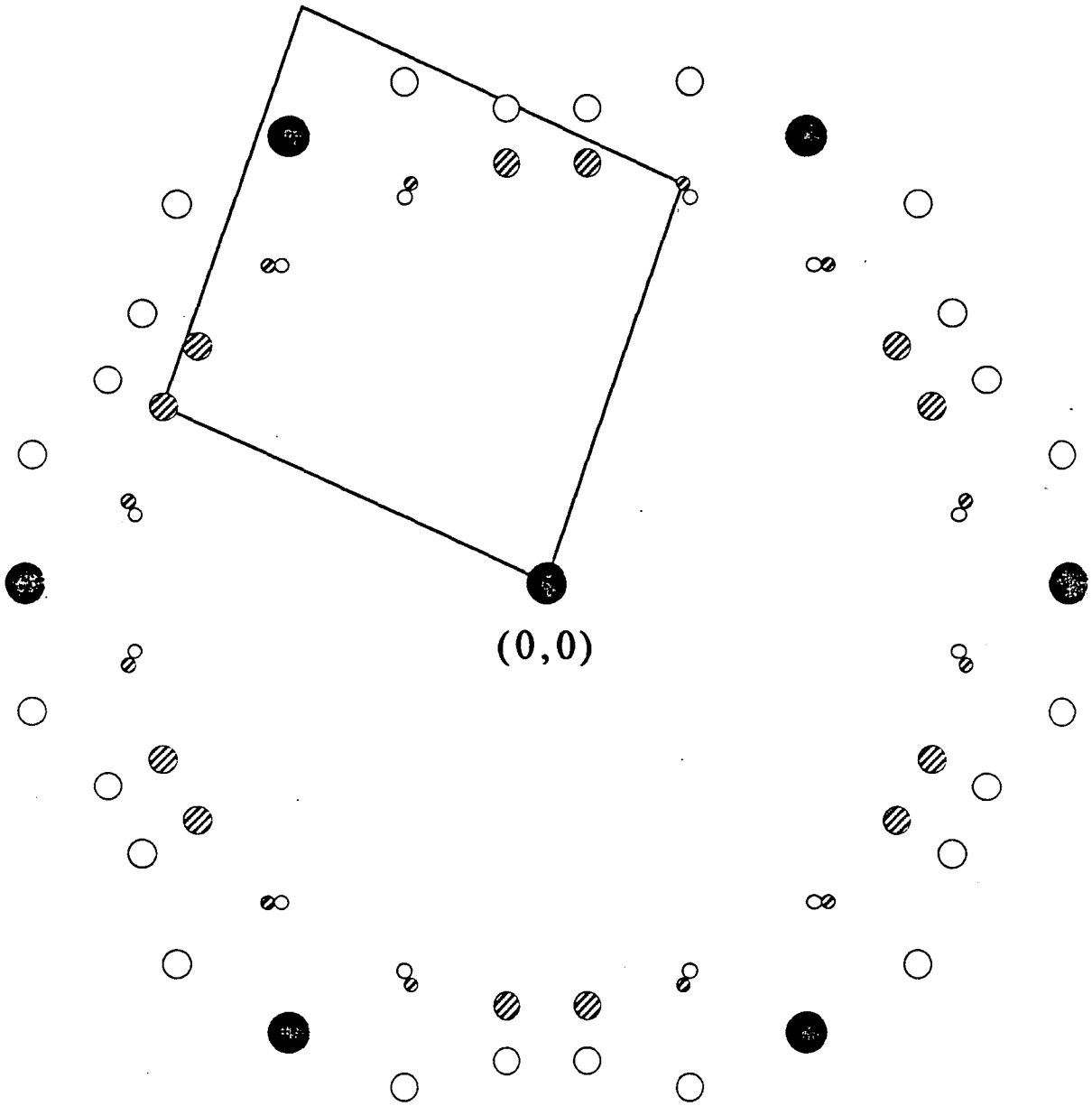

Fig. 5b

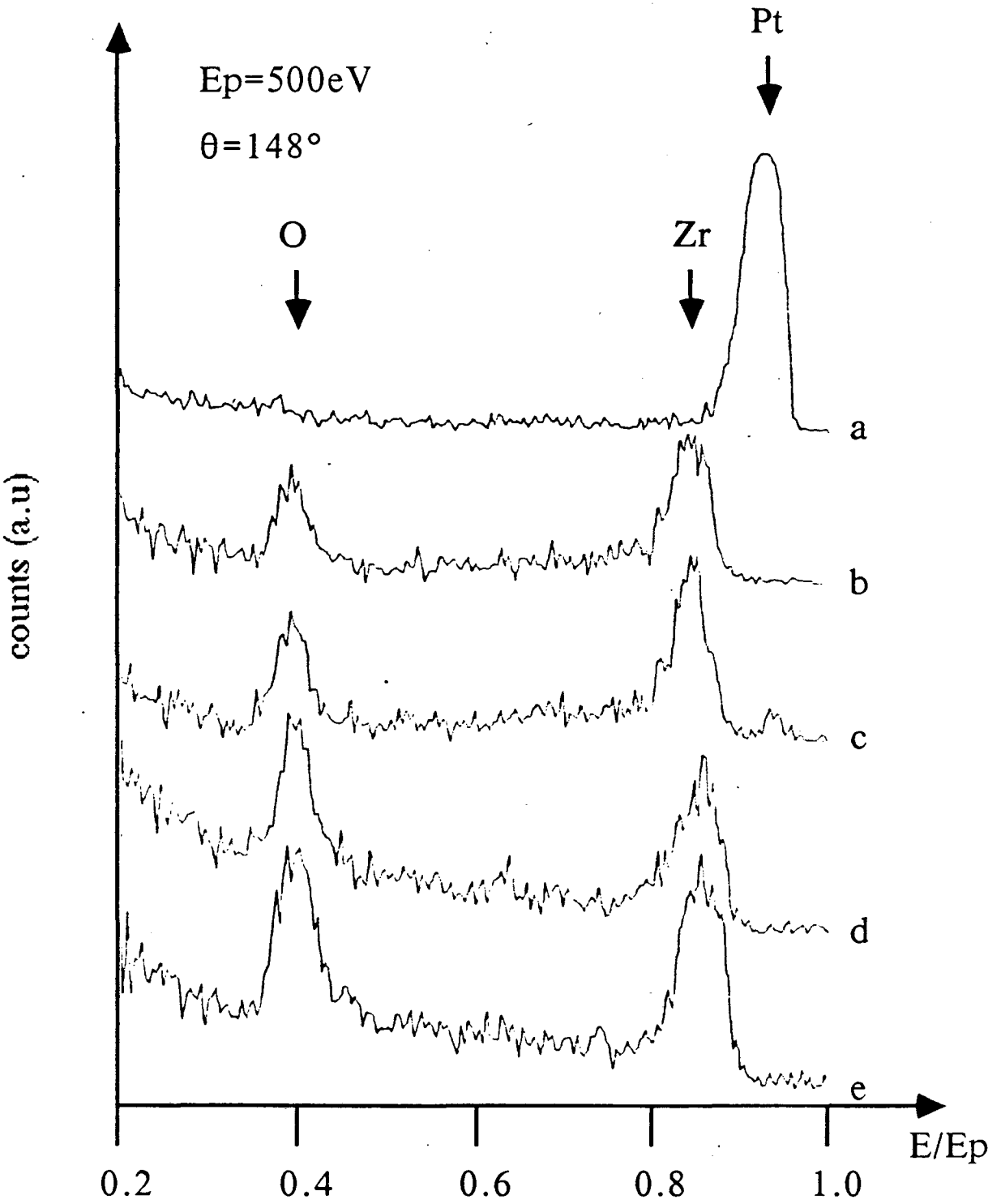

Fig. 6

LAWRENCE BERKELEY LABORATORY
CENTER FOR ADVANCED MATERIALS
1 CYCLOTRON ROAD
BERKELEY, CALIFORNIA 94720